Effect of trap anharmonicity on a free-oscillation atom interferometer

R. H. Leonard and C. A. Sackett

Phys. Rev. A **86**, 043613 — Published 11 October 2012

DOI: 10.1103/PhysRevA.86.043613

Effect of trap anharmonicity on a free-oscillation atom interferometer

R. H. Leonard and C. A. Sackett*

Department of Physics, University of Virginia, Charlottesville, VA 22904

Abstract

A free-oscillation interferometer uses atoms confined in a harmonic trap. Bragg scattering from an off-resonant laser is used to split an atomic wave function into two separated packets. After one or more oscillations in the trap, the wave packets are recombined by a second application of the Bragg laser to close the interferometer. Anharmonicity in the trap potential can lead to a phase shift in the interferometer output. In this paper, analytical expressions for the anharmonic phase are derived at leading order for perturbations of arbitrary power in the position coordinate. The phase generally depends on the initial position and velocity of the atom, which are themselves typically uncertain. This leads to degradation in the interferometer performance, and can be expected to limit the use of a cm-scale device to interaction times of about 0.1 s. Methods to improve performance are discussed.

PACS numbers: 03.75.Dg, 37.25.+k

* sackett@virginia.edu

I. INTRODUCTION

Atom interferometry is a sensitive tool for metrology and probes of fundamental constants [1, 2]. Traditionally it uses atoms in free space, but many groups have investigated interferometry of trapped atoms, both thermal and Bose-condensed [3–12]. The use of confined atoms has several advantages, including the abilities to maintain high density for interaction studies and to impose complex atomic trajectories via the trapping potential. Another significant benefit of confinement is that the atoms do not fall under gravity, so measurements can be extended to long times without requiring a long drop distance.

One interferometer configuration that has been of recent interest is the "free-oscillation" interferometer (Fig. 1), in which atoms are confined in a harmonic trap [9, 11, 13–15]. An off-resonant laser pulse is applied to the atoms and induces momentum kicks via Bragg scattering. Typically, the laser is a standing wave tailored to produce two wave packets with momentum kicks $\pm 2\hbar k$ for light with wavenumber k. The two packets are allowed to separate and complete a half or full oscillation in the trap, at which time the laser pulse is applied again. The fraction of atoms brought back to rest after the second pulse depends on the phase difference between the packets at the time of recombination, making the device an interferometer.

The free-oscillation interferometer can be compared with the Michelson configuration [4, 5, 7, 16], in which the atoms are held in a potential that is nearly flat in one direction. The wave packets are separated in that direction and one or more Bragg reflection pulses are used to reverse the atomic motion and bring the packets back together. The free oscillation interferometer offers several advantages over the Michelson interferometer, chiefly stemming from the difficulty of achieving a perfectly flat potential [13, 15, 17].

However, it is not easy to achieve a perfectly harmonic potential either. Anharmonicity is likely to be an important limit to the performance of a free-oscillation interferometer, because it causes a phase difference between the two arms that depends on the position and velocity of the initial unsplit packet. Thermal atoms will have a large spread in position and velocity, so anharmonicity can be expected to severely limit the usability of a free-oscillation interferometer with non-condensate atoms. Even a Bose-Einstein condensate will have some variation in the initial conditions due to the uncertainty principle, along with extraneous motional excitations from technical effects.

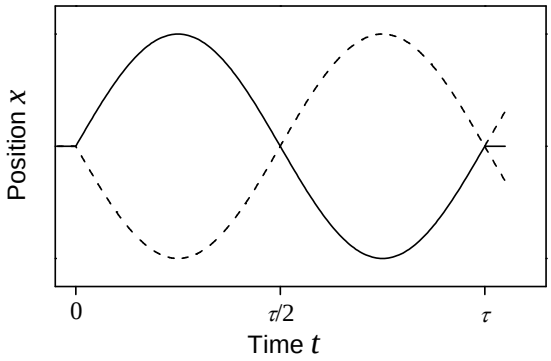

FIG. 1. Atomic trajectories $x(t)$ in a free-oscillation interferometer. Cold atoms are confined in a harmonic potential with period τ. At time $t = 0$ a laser pulse splits the atomic wave function into two packets (solid and dashed curves) moving in opposite directions. After completing either a half or a full oscillation in the trap, the packets are recombined. (A full oscillation is shown.) The fraction of atoms that returns to rest depends on the phase difference developed between the two packets.

In this paper, we calculate the phase shift of a free oscillation interferometer that is induced by anharmonicity. We will ignore atomic interactions here, although they can in fact be important [15]. In Section II we calculate the anharmonic phase shift. In Section III we estimate typical magnitudes of the anharmonicity and suggest some techniques for mitigation of the effect. Finally, Section IV presents concluding remarks.

II. PHASE CALCULATION

A. Perturbative Approach

With reference to the atomic trajectories shown in Fig. 1, we take the atoms to travel along the x direction. We assume this is a principle axis of the trapping potential, and also that anharmonicity does not introduce significant coupling between x and the other directions. In this case, the relevant motion is governed by the one-dimensional Hamiltonian

$$H = \frac{p^2}{2m} + \frac{1}{2}m\omega_0^2 x^2 + mf(x), \tag{1}$$

where m is the atomic mass, $p = m\dot{x}$ the momentum, ω_0 the unperturbed oscillation frequency, and $mf(x)$ is a perturbing potential, assumed to be small.

The phase accumulated by a packet is determined using the classical action [1, 18],

$$\phi(t) - \phi(0) = \frac{1}{\hbar}\int_0^t (T - V)\ dt \tag{2}$$

where the kinetic and potential energies T and V are calculated for the classical trajectory $x_{\text{class}}(t)$. To be precise, this gives the phase of the packet wave function $\psi(x,t)$ at the packet center $\langle x\rangle = x_{\text{class}}$. We here ignore the possible impact of phase gradients across the packet, which require the inclusion of atomic interactions to correctly analyze [13, 15, 17].

The classical trajectory is determined using the equation of motion

$$\ddot{x} + \omega_0^2 x = -\frac{df}{dx}. \tag{3}$$

Perturbative techniques for the solution of (3) are well known [19, 20]. We write $x = x_0 + x_1$ where the subscript indicates the perturbative order. We take $x_0 = A\cos(\omega t - \theta)$, where $\omega = \omega_0 + \omega_1$ includes an amplitude-dependent frequency shift ω_1. Substituting these expressions into (3) and collecting the first-order terms yields

$$\ddot{x_1} + \omega_0^2 x_1 = 2\omega_0\omega_1 x_0 - \left.\frac{df}{dx}\right|_{x_0} \tag{4}$$

The frequency shift ω_1 is determined by requiring that the right-hand side of (4) contain no terms oscillating at ω_0, since these would drive unbounded excitation of x_1. To first order, this yields

$$\omega_1 = \frac{1}{2\pi\omega_0 A}\int_0^{2\pi} \cos u \left.\frac{df}{dx}\right|_{x=A\cos u} du \tag{5}$$

For the interferometer phase shift, we consider the case where atoms make one full oscillation in the potential before recombination, as shown in Fig. 1. The phase developed by a wave packet during this motion is, from (2),

$$\phi = \frac{m}{\hbar}\int_0^\tau \left(\frac{\dot{x}^2}{2} - \frac{\omega_0^2 x^2}{2} - f(x)\right) dt. \tag{6}$$

where τ is the period. Using $x = x_0 + x_1$ and neglecting terms above first order yields

$$\phi_1 = \frac{m}{\hbar}\int_0^\tau \left[\frac{1}{2}\left(\dot{x}_0^2 - \omega_0^2 x_0^2\right) - f(x_0)\right] dt, \tag{7}$$

The terms involving $x_0 x_1$ vanish upon integration because x_0 and x_1 are, by construction, orthogonal on this interval. To first order, the derivative term in (7) can be expressed

$$\dot{x}_0^2 = (\omega_0^2 + 2\omega_0\omega_1)A^2\sin^2(\omega t - \theta). \tag{8}$$

Using this to evaluating the integral leaves a perturbation phase

$$\phi_1 = \frac{\pi m}{\hbar} A^2 \omega_1 - \frac{m}{\hbar} \int_0^\tau f(x_0)\, dt. \tag{9}$$

Two cases can now be considered. The first supposes that $f(x)$ varies over a length scale small compared to the amplitude of the atomic motion A. This might be caused by speckle in a laser trap or roughness in the conductors of a magnetic chip trap. In this case, ω_1 will be small because df/dx in Eq. (5) will rapidly oscillate. In this limit, the phase shift will be dominated by the second term in (9), which is simply the integral of the perturbing potential:

$$\phi_1 \to -\frac{m}{\hbar} \int_0^\tau f(x_0)\, dt. \tag{10}$$

Further analysis would require knowing $f(x)$, which will in general be specific to a particular apparatus.

The second case supposes that $f(x)$ is slowly varying compared to the atomic amplitude. This might result when the confinement potential is created by a distant magnetic or optical element. Here it is reasonable to Taylor expand $f(x)$ as a power series

$$f(x) \to \sum_{n=3}^{\infty} f_n \left(\frac{x}{R}\right)^n \tag{11}$$

where R is a characteristic length scale, which can typically be taken as the distance to the trapping element. If $x \ll R$, the dominant term will be the lowest power of n for which f_n is non-vanishing. In a symmetric trap, f_n will be suppressed for all odd n, and deliberate design may result in the suppression of f_n for one or more even n as well. In general, however, ω_1 will be non-zero and both terms of Eq. (9) will contribute. This case corresponds to the conventional anharmonic oscillator, and it is the main focus of the present paper. We continue its analysis in Section II B below.

In the intermediate case, where the length scale of f is comparable to A, the effect on the phase is complicated. If the detailed form of $f(x)$ is known, then Eqs. (5) and (9) can be used to numerically estimate the phase shift. However, direct numerical computation of Eq. (2) would require similar effort and give greater accuracy.

B. Anharmonic Trap: First Order

As explained above, we here consider the case of a power-law perturbation which we will express as

$$f(x) = \frac{1}{n}\lambda_n x^n \tag{12}$$

If n is odd, the result is simple: ω_1 in Eq. (5) and ϕ in Eq. (9) are both zero by symmetry. There is thus no first order effect on the interferometer, but we will consider the second order effect in Section II C.

If n is even, then the frequency shift can be expressed as

$$\omega_1 = \frac{\lambda_n}{2\pi} A^{n-2} \int_0^\tau \cos^n(\omega t - \theta)\, dt = \frac{\lambda_n}{\omega_0} A^{n-2} h_n \tag{13}$$

where

$$h_n = \frac{1}{2\pi}\int_0^{2\pi} \cos^n u\, du = \frac{n!}{(n!!)^2}. \tag{14}$$

Using this in Eq. (9) yields a trajectory phase

$$\phi_1^{(n)} = \left(1 - \frac{2}{n}\right)\frac{\pi m}{\hbar\omega_0} A^n \lambda h_n \qquad (n \text{ even}). \tag{15}$$

Equation (15) gives the first order phase acquired by a wave packet during one complete orbit through the confining potential. However, in the actual interferometer, neither packet makes a perfectly complete orbit. Suppose the wave packet starts at mean position x_a and mean velocity v_a. It will be convenient to work with the scaled velocity $u_a \equiv v_a/\omega_0$. The initial packet is split into two, with one packet acquiring a velocity impulse $+u_0 = 2\hbar k/(m\omega_0)$ and the other $-u_0$. The two packets therefore have motional amplitudes $A_\pm$ given by $A_\pm^2 = x_a^2 + u_a^2 + u_0^2 \pm 2u_a u_0$. Because these amplitudes are different, the packets will experience different motional frequencies $\omega_\pm = \omega_0 + \omega_{1\pm}$. The interferometer will be complete when the two packets cross at time t_c, with $x_+(t_c) = x_-(t_c)$. The crossing time is approximately equal to the periods for the two packets, but differs by small amounts $\delta t_\pm = t_c - 2\pi/\omega_\pm$. In terms of the frequency shifts $\omega_{1\pm}$, this implies

$$\delta t_+ - \delta t_- = \frac{2\pi}{\omega_0^2}\left(\omega_{1+} - \omega_{1-}\right). \tag{16}$$

Since the δt's are already first order in λ_n, their effect on the trajectories and phases can be calculated in zeroth order. The trajectory is $x_\pm(t) = x_a \cos\omega_\pm t + (u_a \pm u_0)\sin\omega_\pm t$, so

setting $x_+ = x_-$ at t_c yields $(u_a + u_0)\delta t_+ = (u_a - u_0)\delta t_-$, leading to

$$\delta t_\pm = \frac{\pi \lambda_n h_n}{\omega_0^3} \left(-\frac{u_a}{u_0} \pm 1 \right) \left(A_+^{n-2} - A_-^{n-2} \right). \tag{17}$$

The zero-order phase shift developed over a short time δt is readily calculated from the action to be

$$\delta\phi = -\frac{m\omega_0^2}{2\hbar} A^2 \delta t \cos 2\theta. \tag{18}$$

Here $A_\pm^2 \cos 2\theta_\pm = x_a^2 - (u_a \pm u_0)^2$. The additional phase difference from the trajectories is then

$$\delta\phi_+ - \delta\phi_- = -\frac{\pi m \lambda_n h_n}{\hbar\omega_0} (A_+^{n-2} - A_-^{n-2})(x_a^2 + u_a^2 - u_0^2) \tag{19}$$

This adds to the the result (15) to give the total anharmonic phase for a full-cycle interferometer,

$$\begin{aligned} \Delta\phi_1^{(n)} &= \phi_{1+}^{(n)} + \delta\phi_+ - \phi_{1-}^{(n)} - \delta\phi_- \qquad (n \text{ even}) \\ &= \frac{\pi m \lambda_n h_n}{\hbar\omega_0} \left[\left(1 - \frac{2}{n} \right) \left(A_+^n - A_-^n \right) \right. \\ &\qquad \left. - \left(x_a^2 + u_a^2 - u_0^2 \right) \left(A_+^{n-2} - A_-^{n-2} \right) \right]. \end{aligned} \tag{20}$$

We note that in practice, the determination of t_c is subject to experimental uncertainty, which can lead to additional phase shifts. This issue is discussed further in Section III C below.

From Eq. (20), the first order anharmonic effect can be calculated for any power n. In particular, it is evident that a nonzero phase shift can be obtained only when $v_a = \omega_0 u_a$ is nonzero, since otherwise the amplitudes A_+ and A_- will be equal and both packets will trace out the same orbit through the trap. The same argument can be made for the the more general result of Eq. (9).

The values of n most likely to be of interest are 4 and 6. Evaluating (20) for these cases yields

$$\Delta\phi_1^{(4)} = 3\pi \frac{m\lambda_4}{\hbar\omega_0} u_0^3 u_a \tag{21}$$

and

$$\Delta\phi_1^{(6)} = 5\pi \frac{m\lambda_6}{\hbar\omega_0} u_0^3 u_a (x_a^2 + u_a^2 + u_0^2). \tag{22}$$

We checked these calculations by comparing to numerical integration of the action (6) using the exact equation of motion (3). Figure 2 shows a comparison of the numerical and analytical results. In all cases examined, we found good agreement.

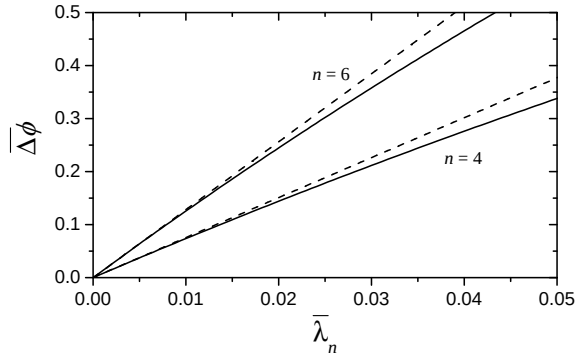

FIG. 2. Comparison of first-order analysis (dashed curves) to numerical calculation (solid curves) of the anharmonic phase shifts in a free-oscillation interferometer. Here $\overline{\Delta\phi} = (\omega_0/\omega_r)\Delta\phi$, with $\Delta\phi$ from (20). The recoil frequency for the Bragg laser beam is $\omega_r = mv_0^2/8\hbar$. The dimensionless anharmonic coefficient $\overline{\lambda}_n$ is given by $\lambda_n v_0^{n-2}/\omega_0^n$. The curves are labeled with the power of the anharmonic perturbation n. Both cases shown use $v_a = 0.1v_0$ and $x_a = 0.1v_0/\omega_0$.

C. Anharmonic Trap: Second-Order

As noted previously, there is no first-order phase shift for a power-law perturbation with odd power n. However, if an odd-n coefficient λ_n is relatively large, the second-order effect from it could be comparable to the first-order effect from an even power at higher n. In particular, terms scaling with $(\lambda_3)^2$ have the same amplitude dependence as those scaling with λ_4, so a second-order calculation of the odd-n terms is needed to make a fair comparison of their impact.

To proceed, we shall require the order-one correction to the motion, x_1. Its equation of motion is

$$\ddot{x_1} + \omega_0^2 x_1 = -\lambda_n A^{n-1} \cos^{n-1}(\omega_0 t - \theta). \tag{23}$$

The cosine term here can be expanded using

$$(\cos u)^p = \sum_s^p h_s^{(p)} \cos su, \tag{24}$$

where the sum is over odd s from 1 to p when p is odd, and over even s from 0 to p when p

is even. The expansion coefficients are

$$h_s^{(p)} = \frac{p!}{(p+s)!!(p-s)!!}(2-\delta_{s0}). \tag{25}$$

Here $h_0^{(n)}$ is identical to h_n in Eq. (14). The solution to (23) is then

$$x_1 = \frac{\lambda_n A^{n-1}}{\omega_0^2} \sum_{\text{even } s}^{n-1} \frac{h_s^{(n-1)}}{s^2-1} \cos s(\omega_0 t - \theta). \tag{26}$$

For later use, we note that the same result holds for even n, except that $\omega_0 \to \omega$ and the sum is over odd $s > 1$.

Extending the perturbation series to second order, we have $x = x_0 + x_1 + x_2$ with $\omega = \omega_0 + \omega_2$. Inserting into the equation of motion (3) and collecting second order terms gives

$$\begin{aligned} \ddot{x_2} + \omega_0^2 x_2 = &-(n-1)\lambda x_1 A^{n-2} \cos^{n-2}(\omega_0 t - \theta) \\ &+ 2\omega_0\omega_2 A \cos(\omega_0 t - \theta). \end{aligned} \tag{27}$$

Again, the right-hand side must have no ω_0 components. After some manipulation, this leads to

$$\omega_2 = \frac{(n-1)\lambda_n^2 A^{2n-4}}{2\omega_0^3} \sum_{\text{even } s}^{n-1} \frac{[h_s^{(n-1)}]^2}{s^2-1}(1+\delta_{s0}). \tag{28}$$

To calculate the phase shift, we expand the Lagrangian to second order and discard terms that trivially integrate to zero. This yields

$$\begin{aligned} \phi_2^{(n)} = \frac{m}{\hbar} \int_0^\tau \Bigg[&\frac{1}{2}\left(\dot{x}_0^2 - \omega_0^2 x_0^2\right) \\ &+ \frac{1}{2}\left(\dot{x}_1^2 - \omega_0^2 x_1^2\right) - \lambda_n x_0^{n-1} x_1 \Bigg]\, dt. \end{aligned} \tag{29}$$

The first pair of terms are evaluated just as for even n to give a contribution $\phi_A = \pi m A^2 \omega_2/\hbar$. The second pair of terms can be evaluated using expression (26) and orthogonality to obtain

$$\begin{aligned} \phi_B &= -\frac{\pi}{2}\frac{m\lambda^2 A^{2n-2}}{\hbar\omega_0^3} \sum_{\text{even } s}^{n-1} \frac{[h_s^{(n-1)}]^2}{1-s^2}(1+\delta_{s0}) \\ &= \frac{\pi}{n-1}\frac{mA^2\omega_2}{\hbar}. \end{aligned} \tag{30}$$

The final term can evaluated similarly by expanding the $\cos^{n-1}(\omega_0 t - \theta)$ factor to yield

$$\phi_C = -\frac{2\pi}{n-1}\frac{mA^2\omega_2}{\hbar}. \tag{31}$$

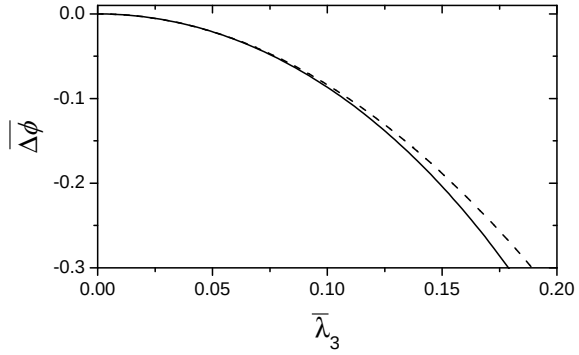

FIG. 3. Comparison of leading-order analysis (dashed) to numerical calculation (solid) of the $n = 3$ anharmonic phase. The dimensionless quantities $\overline{\Delta\phi}$ and $\overline{\lambda}_3$ are defined as in Fig. 2, with $\Delta\phi$ from Eq. (34). The calculation uses $v_a = 0.1v_0$ and $x_a = 0.1v_0/\omega_0$.

Combining these three terms gives the net phase for odd n,

$$\phi_2^{(n)} = \frac{\pi(n-2)}{n-1}\frac{mA^2\omega_2}{\hbar} \qquad (n \text{ odd}). \tag{32}$$

with ω_2 from Eq. (28).

To (32) must be added the correction $\delta\phi$ accounting for the difference in oscillation frequencies for the two trajectories in the interferometer. This proceeds exactly as for even n. In fact, the leading order phase shift for any n can be expressed as

$$\Delta\phi^{(n)} = \frac{\pi m}{\hbar}\Big[c_n\left(\delta\omega_+ A_+^2 - \delta\omega_- A_-^2\right) - \left(x_a^2 + u_a^2 - u_0^2\right)\left(\delta\omega_+ - \delta\omega_-\right)\Big] \tag{33}$$

where for even n, $c_n = (n-2)/n$ and $\delta\omega = \omega_1$, while for odd n, $c_n = (n-2)/(n-1)$ and $\delta\omega = \omega_2$. The most interesting odd case $n = 3$ gives

$$\Delta\phi_2^{(3)} = -\frac{10\pi}{3}\frac{m\lambda_3^2}{\hbar\omega_0^3}u_0^3 u_a, \tag{34}$$

similar to Eq. (21) as claimed. We again checked this result against direct numerical calculation of the phase, and found good agreement as seen in Fig. 3.

In principle, the analytical approach used here could be continued to provide the next-leading-order correction to the phase. However, the calculation rapidly becomes complicated

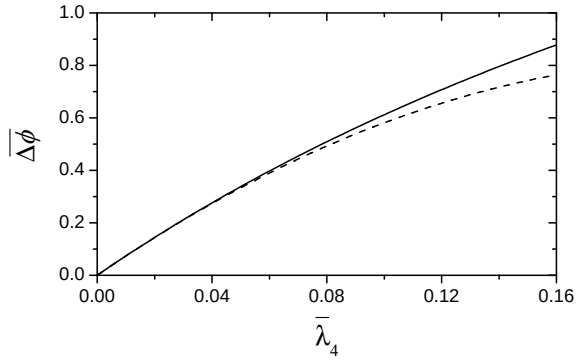

FIG. 4. Comparison of second-order fit (dashed curves) to numerical calculation (solid curves) for a full-cycle interferometer with quartic ($n = 4$) anharmonicity. Plotted values are scaled as in Fig. 2, with $\Delta\phi$ from Eqs. (21) and (35) using $v_a = 0.1v_0$ and $x_a = 0.1v_0/\omega_0$.

[21, 22]. We did, however, numerically investigate the second-order correction for the quartic potential, as this seems the case most likely to have practical importance. We find a net interferometer phase of

$$\Delta\phi_2^{(4)} = -K\frac{m\lambda_4^2}{\hbar\omega_0^3}u_0^3u_a\left(u_0^2 + \kappa_1 u_a^2 + \kappa_2 x_a^2 + \kappa_3 x_a u_a\right) \tag{35}$$

with dimensionless $K = 20.61$, $\kappa_1 = 1.667$, $\kappa_2 = 1.001$, and $\kappa_3 = 2.157$. The estimated accuracy for $\Delta\phi_2$ is 0.2%, based on the consistency of the fit across a range of parameter values. Figure 4 shows an example comparison including both first and second order contributions. We note that (22) and (35) have similar scaling with amplitude, so if neither λ_4 nor λ_6 are suppressed, both terms must be considered if this level of accuracy is required.

D. Half-Cycle Interferometer

Until now we have supposed the atoms to complete a (nearly) full oscillation in the trap. An interferometer can also be implemented using just one half oscillation, with the packets recombined at $t = \tau/2$ in Fig. 1. Here the phase will clearly be more sensitive to asymmetries in the confining potential, but it also becomes sensitive to asymmetric effects that might be of interest. It is worth noting, however, that a half-cycle interferometer remains insensitive to uniform static forces like gravity, since a constant force will simply shift the center of the

harmonic potential with no effect on the trajectories or phase.

For even n, the phase calculation proceeds just as in the full-oscillation case, but all terms are reduced in magnitude by a factor of two. The final phase shift is therefore just one half of Eq. (20).

The effect of odd anharmonicities change more significantly, as expected. There is now a first-order contribution to the phase,

$$\phi_{\rm half}^{(n)} = -\frac{m}{\hbar}\int_0^{\tau/2} \frac{\lambda_n}{n} x_0^n \, dt \tag{36}$$

that is readily evaluated to

$$\phi_{\rm half}^{(n)} = -\frac{2m\lambda_n}{n\hbar\omega_0} h_1^{(n)} A^n \sin\theta. \tag{37}$$

To this order, there is no correction to the oscillation frequency, so $\phi_{\rm half}^{(n)}$ is the only contribution to the interferometer phase difference. Here $A_\pm \sin\theta_\pm = u_a \pm u_0$. Evaluating $\phi_{\rm half}$ for the case $n = 3$ yields

$$\Delta\phi_{\rm half}^{(3)} = -\frac{2m\lambda_3}{\hbar\omega_0} u_0 \left(u_0^2 + x_a^2 + 3u_a^2\right). \tag{38}$$

Here the lack of symmetry means that a non-zero effect is obtained even for $u_a = 0$.

III. DISCUSSION AND IMPACT

A. Estimation of Effect

Evaluating the anharmonic phase shift for a particular experiment obviously requires knowing the value of the lowest-power unsuppressed λ_n coefficient, either by measurement or by calculation from the trap geometry. Typically, however, an order-of-magnitude estimate for λ_n can be obtained from the power series expansion of Eq. (11). For the appropriate length scale R, the coefficients f_n in that expansion should have comparable magnitudes. Furthermore, in the typical case that the harmonic confinement is provided by the same elements that introduce $f(x)$, the expansion could be extended to $n = 2$ and the f_2 coefficient, given by $f_2 = \omega_0^2 R^2/2$, will have comparable magnitude to the other f_n's. In terms of the λ_n coefficients of Eq. (12), this implies

$$\lambda_n \approx \frac{n\omega_0^2}{2R^{n-2}}. \tag{39}$$

This provides a useful guide to when anharmonic effects are likely to be important. For instance, a symmetric trap (with $\lambda_{\text{odd}} \approx 0$) would have

$$\Delta\phi_1^{(4)} \approx 6\pi \frac{m v_a v_0^3}{\hbar \omega_0^3 R^2} \tag{40}$$

Using Rb atoms with $\omega_0 = 2\pi \times 10$ Hz, $v_0 = 1.2$ cm/s, and $R = 1$ cm, maintaining $\Delta\phi \ll 1$ requires the initial atomic velocity $v_a \ll 0.5$ mm/s. The same configuration with ω_0 reduced to $2\pi \times 1$ Hz would require $v_a \ll 0.5$ μm/s. The strong dependence on ω_0 reflects the fact that a weaker trap will allow the atomic trajectories to extend to larger distances where the anharmonicity is more significant.

In principle, a fixed phase shift could be measured and subtracted out, but in practice v_a is likely to fluctuate, making the anharmonicity into a source of noise. For thermal atoms, the velocity spread will be determined by the gas temperature, while for condensate atoms it is limited by the uncertainty principle and technical effects. In our experiments [23], we produce Rb condensates in a relatively tight trap and then adiabatically reduce the confinement to give an oscillation frequency in the range of 1 to 10 Hz. After this process, we typically observe a center-of-mass motional excitation corresponding to a velocity variance σ_v^2 of about $\omega_0 \times 10^{-8}$ m^2/s. We attribute this to a combination of imperfect adiabaticity, forces from uncontrolled ambient magnetic fields, and mechanical vibrations of the apparatus. In comparison, the non-interacting harmonic oscillator ground state has $\sigma_v^2/\omega_0 = \hbar/m = 7.3 \times 10^{-10}$ m^2/s. The fundamental velocity uncertainty can be even lower in an interacting condensate [24], but the interplay between anharmonicity and interactions requires additional consideration beyond the scope of this work.

In practice, then, anharmonic effects can be expected to limit the usable oscillation frequency for a given trap geometry, and thus the measurement time τ of the interferometer. In the case of quartic anharmonicity with our empirical σ_v, the phase fluctuations will reach one radian at $\tau \approx (0.09 \text{ s}) R^{4/5}$, for R in cm. This increases by about a factor of two for the ideal ground state σ_v. Anharmonic effects can thus be expected to impact a cm-scale device operating with interaction times greater than about 0.1 s.

B. Amelioration

An obvious way to reduce the impact of trap anharmonicity is to reduce the anharmonicity itself by using a larger trap geometry to increase R. However, practical applications often favor a more compact apparatus. Also, in both magnetic and optical traps the electrical or optical power required increases rapidly with the trap size.

Alternatively, a small trap could be designed with reduced anharmonicity. Typically this would be achieved by tuning one or more λ_n coefficients to zero. For example, with our empirical σ_v a trap with $\lambda_4 \approx 0$ and $\lambda_6 \approx 3\omega_0^2/R^4$ would give one radian of phase noise at $\tau \approx (0.5\text{ s})R^{8/9}$, again with R in cm. This is about five times better than obtained with unsuppressed λ_4. Controlling many coefficients in this manner, however, is likely to be challenging.

We propose here another possibility for controlling anharmonic effects, the use of a dual interferometer as illustrated in Fig. 5. Here a wave packet initially at (x_a, v_a) is split and allowed to propagate for one quarter oscillation, after which the packets will be nearly at rest, with residual velocities $v \approx -\omega_0 x_a$ for both. These packets are used as the sources for two independent interferometers: the packets are split, allowed to oscillate for one period, and then recombined. The output signal Ψ is taken as the difference between the phases of two interferometers. Because the initial velocities of the two interferometers are correlated, the leading-order anharmonic phases cancel in the difference. The phase difference is also less sensitive to mechanical vibrations and several other technical effects [25]. However, this configuration evidently requires the phase shift of metrological interest to be differential between the two interferometers. For example, a local field might be applied to just a single packet.

We analyze the dual interferometer for the $n = 4$ case. The trajectories are, from Eq. (26),

$$x(t) = A\cos(\omega t - \theta) + \frac{\lambda_4}{32\omega_0^2}A^3\cos 3(\omega t - \theta). \tag{41}$$

We use this solution to determine the actual initial conditions for the subsequent pair of interferometers. We here use + (−) to label the interferometer derived from the packet originally given a positive (negative) momentum kick.

The amplitudes and angles in (41) must be determined in terms of $x_\pm(0) = x_a$ and $u_\pm(0) = u_a \pm u_0$. We write $A = A_0 + A_1$ and $\theta = \theta_0 + \theta_1$. In zeroth order, we have

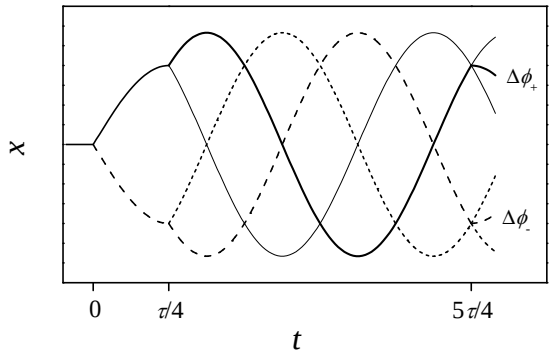

FIG. 5. Dual interferometer configuration. At time $t = 0$, a Bragg splitting pulse is applied to the nominally stationary initial wave packet in a nominally harmonic trap of period τ. The resulting two packets move in the potential until the come to nominal rest at time $\tau/4$, when the splitting pulse is again applied. This produces two pairs of packets. All four packets are allowed to propagate for a measurement time τ and then recombined with a final pulse. The upper pair of trajectories (solid curves) forms one interferometer with output phase $\Delta\phi_+$, and the lower pair (dashed curves) forms another with output phase $\Delta\phi_-$. The phase difference $\Psi = \Delta\phi_+ - \Delta\phi_-$ features reduced sensitivity to the anharmonicity of the trap potential.

$x_a = A_{0\pm}\cos\theta_{0\pm}$ and $u_a \pm u_0 = A_{0\pm}\sin\theta_{0\pm}$. The first order corrections are then calculated to be

$$A_{1\pm} = \frac{1}{32}\frac{\lambda_4 A_{0\pm}^3}{\omega_0^2}\left(8\cos^4\theta_{0\pm} - 9\right). \tag{42}$$

and

$$\theta_{1\pm} = -\frac{1}{8}\frac{\lambda_4}{\omega_0^2}A_{0\pm}^2\cos\theta_{0\pm}\sin\theta_{0\pm}\left(3 + 2\cos^2\theta_{0\pm}\right). \tag{43}$$

The frequencies $\omega_\pm$ are given by (13),

$$\omega_\pm = \omega_0 + \frac{3\lambda_4}{8\omega_0}A_{0\pm}^2. \tag{44}$$

After the first splitting pulse, the packets propagate for a time $t_b = \pi/(2\bar{\omega})$, where $\bar{\omega} = (\omega_+ + \omega_-)/2$. Inserting this into the above trajectories yields

$$\begin{aligned} u_\pm(t_b) = -x_a - \frac{\lambda_4}{8\omega_0^2}\big[&3\pi u_a u_0\left(u_0 \pm u_a\right) \\ &+2x_a\left(3u_0^2 + 3u_a^2 + x_a^2 \pm 6u_0u_a\right)\big]. \end{aligned} \tag{45}$$

Using these as the initial velocities for the two subsequent interferometers in (21) gives a phase difference

$$\Psi \equiv \Delta\phi_+ - \Delta\phi_- = -\frac{9\pi}{4}\frac{m\lambda_4^2}{\hbar\omega_0^3}u_0^4 u_a(\pi u_a + 4x_a), \tag{46}$$

which is much smaller than the individual $\Delta\phi$'s. The result is second-order in λ_4, but the direct second-order effect of (35) also largely cancels to give a third-order correction to Ψ. The leading-order λ_6 effect (22) cancels as well. Using the estimated value $\lambda_4 \approx 2\omega_0^2/R^2$, our empirical values for σ_v, and taking $\sigma_x \approx \sigma_v/\omega_0$, we obtain a measurement time limit $\tau \approx 0.9R$ s/cm for $\sigma_\Psi < 1$.

C. Measurement of Anharmonicity

Although the estimates above may be helpful, an accurate consideration of the effects discussed here will require actual knowledge of the relevant anharmonic coefficients. While they can be calculated in principle, an experimental technique to measure them would likely be useful. The most straightforward approach is to observe how the oscillation frequency depends on the motional amplitude, via $\delta\omega$. However, it may be difficult to measure $\delta\omega$ with sufficient accuracy. For example, in a 10-Hz trap with quartic anharmonicity and $R = 1$ cm ($\lambda_4 = 8\times10^3$ cm^{-2} s^{-2}), Rb atoms with $v_a = 0.5$ mm/s would experience a significant phase $\Delta\phi \approx 1$ rad. However, the frequency shift for atoms with amplitude $A = v_0/\omega_0 \approx 200$ μm would be only 3 mHz. Such a small shift could be difficult to measure, given a finite lifetime of atoms in the trap. It may prove more effective to use the interferometer to characterize the trap, by for instance measuring how the interference phase $\Delta\phi$ varies with v_a. The results presented here should be useful for this purpose as well.

It should also be noted that imprecise knowledge of the oscillation frequency ω can itself lead to phase uncertainty. In deriving (20), we assumed a measurement time t_c such that the two packet centers exactly crossed at the time of recombination. If the actual measurement time is too far from t_c, the interference contrast will be reduced because the packets will not be well-overlapped. For a small timing error, however, the overlap will remain large and the dominant effect will be a phase shift resulting from the differing velocities of the two packets. This can be calculated from Eq. (18) along with a correction $mv_a\delta x/\hbar$ for packet separation δx. The result is

$$\delta\phi = 2\frac{m}{\hbar}v_0 v_a \delta t \tag{47}$$

for timing error $\delta t = t - t_c$. Using our empirical value for the velocity uncertainty in Rb, this results in a significant phase uncertainty of 7 rad per ms of timing error. As above, determining ω with sufficient accuracy to avoid this problem may be challenging. This phase error can be reduced using the dual interferometer scheme, because to lowest order it is the same for both pairs of trajectories.

IV. CONCLUSIONS

We have calculated the leading-order effects of trap anharmonicity on a free-oscillation atom interferometer. For a typical cm-scale device, anharmonic phase shifts are likely to be important for interaction times of about 0.1 s or greater, with the effects growing rapidly as the interaction time is increased. Possible methods for amelioration include nulling the low-order anharmonic coefficients via careful trap design, using a larger-scale trap with less anharmonicity, minimization of the initial velocity of the atoms, or phase cancellation in a dual interferometer.

ACKNOWLEDGMENTS

This work was supported by the National Science Foundation (Grant No. PHY- 0244871).

---

[1] P. R. Berman, ed., *Atom Interferometry* (Academic Press, San Diego, 1997).

[2] A. D. Cronin, J. Schmiedmayer, and D. E. Pritchard, Rev. Mod. Phys. **81**, 1051 (2009).

[3] Y. Shin, M. Saba, T. A. Pasquini, W. Ketterle, D. E. Pritchard, and A. E. Leanhardt, Phys. Rev. Lett. **92**, 050405 (2004).

[4] Y. J. Wang, D. Z. Anderson, V. M. Bright, E. A. Cornell, Q. Diot, T. Kishimoto, M. Prentiss, R. A. Saravanan, S. R. Segal, and S. Wu, Phys. Rev. Lett. **94**, 090405 (2005).

[5] S. Wu, E. J. Su, and M. Prentiss, Euro. Phys. J. D **35**, 111 (2005).

[6] T. Schumm, S. Hofferberth, L. M. Andersson, S. Wildermuth, S. Groth, I. Bar-Joseph, J. Schmiedmayer, and P. Krüger, Nat. Phys. **1**, 57 (2005).

[7] O. Garcia, B. Deissler, K. J. Hughes, J. M. Reeves, and C. A. Sackett, Phys. Rev. A **74**, 031601(R) (2006).

[8] A. S. Arnold, C. S. Garvie, and E. Riis, Phys. Rev. A **73**, 041606(R) (2006).

[9] M. Horikoshi and K. Nakagawa, Phys. Rev. Lett. **99**, 180401 (2007).

[10] R. E. Sapiro, R. Zhang, and G. Raithel, Phys. Rev A **79**, 043630 (2009).

[11] P. M. Baker, J. A. Stickney, M. B. Squires, J. A. Scoville, E. J. Carlson, W. R. Buchwald, and S. M. Miller, Phys. Rev. A **80**, 063615 (2009).

[12] F. Baumgärtner, R. J. Sewell, S. Eriksson, I. Llorente-Garcia, J. Dingjan, J. P. Cotter, and E. A. Hinds, Phys. Rev. Lett. **105**, 243003 (2010).

[13] J. H. T. Burke, B. Deissler, K. J. Hughes, and C. A. Sackett, Phys. Rev. A. **78**, 023619 (2008).

[14] S. R. Segal, Q. Diot, E. A. Cornell, A. A. Zozulya, and D. Z. Anderson, Phys. Rev. A **81**, 053601 (2010).

[15] R. P. Kafle, D. Z. Anderson, and A. A. Zozulya, Phys. Rev. A **84**, 033639 (2011).

[16] J. A. Stickney, R. P. Kafle, D. Z. Anderson, and A. A. Zozulya, Phys. Rev. A **77**, 043604 (2008).

[17] M. Olshanii and V. Dunjko (2005), arXiv: cond-mat/0505358.

[18] P. Storey and C. Cohen-Tannoudji, J. Phys. II France **4**, 1999 (1994).

[19] L. D. Landau and E. M. Lifschitz, *Mechanics* (Pergammon Press, Oxford, 1976), 3rd ed.

[20] V. Barger and M. Olsson, *Classical mechanics: a modern perspective* (McGraw-Hill, New York, 1995), 2nd ed.

[21] C. R. Eminhizer, R. H. G. Helleman, and E. W. Montroll, J. Math. Phys. **17**, 121 (1976).

[22] A. I. Kuznetsov, O. V. Karagioz, and V. P. Izmailov, Meas. Tech. **48**, 848 (2005).

[23] J. M. Reeves, O. Garcia, B. Deissler, K. L. Baranowski, K. J. Hughes, and C. A. Sackett, Phys. Rev. A **72**, 051605(R) (2005).

[24] J. Stenger, S. Inouye, A. P. Chikkatur, D. M. Stamper-Kurn, D. E. Pritchard, and W. Ketterle, Phys. Rev. Lett. **82**, 4569 (1999).

[25] G. T. Foster, J. B. Fixler, J. M. McGuirk, and M. A. Kasevich, Opt. Lett. **27**, 951 (2002).